SUPPLEMENTAL DATA

Dysregulation of $GABA_A$ receptor-mediated neurotransmission during the auditory cortex critical period in the Fragile X syndrome mouse model

Yeri J. Song, Bo Xing, Aaron J. Barbour, Chengwen Zhou, Frances E. Jensen

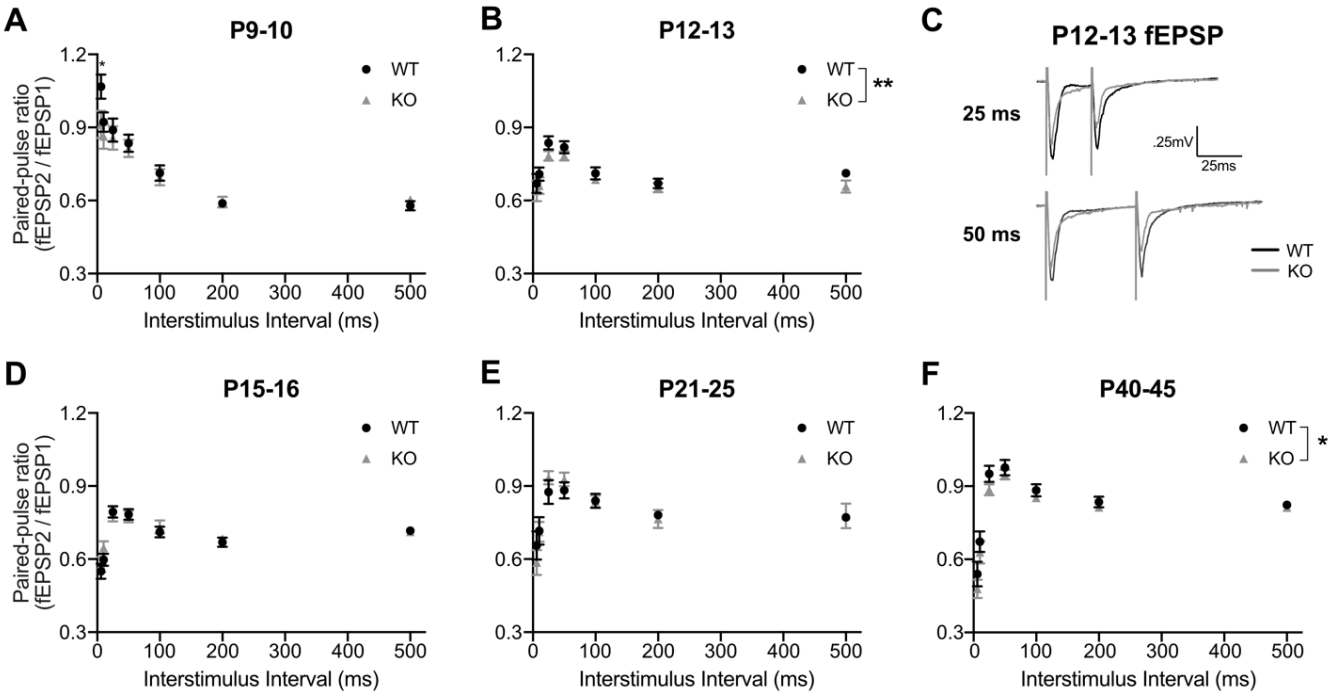

Supplemental Figure 1. Altered presynaptic regulation of L4-L2/3 auditory cortex circuit in P12 *Fmr1* KO mice. (A-F) Paired-pulse ratios (PPR) from MEA fEPSP recordings across developmental ages to measure differences in short-term plasticity driven by presynaptic mechanisms. L4-L2/3 largely have short-term depression (PPR < 1). *Fmr1* KO mice exhibit a significant difference in PPRs at (B) P12-13 (2-way ANOVA, genotype, $F_{(1,300)}$ = 7.007, p = 0.0085), and (F) P40-45 (2-way ANOVA, genotype, $F_{(1,175)}$ = 5.138, p = 0.025), with a trend towards more depressed PPR values particularly at 25, 50, and 500 ms. (C) Representative fEPSP traces at P12-13 of interstimulus intervals of 25 and 50 ms. The number of slices and mice analyzed for each age and genotype are reported in Figure 1. * p < 0.05, ** p < 0.01.

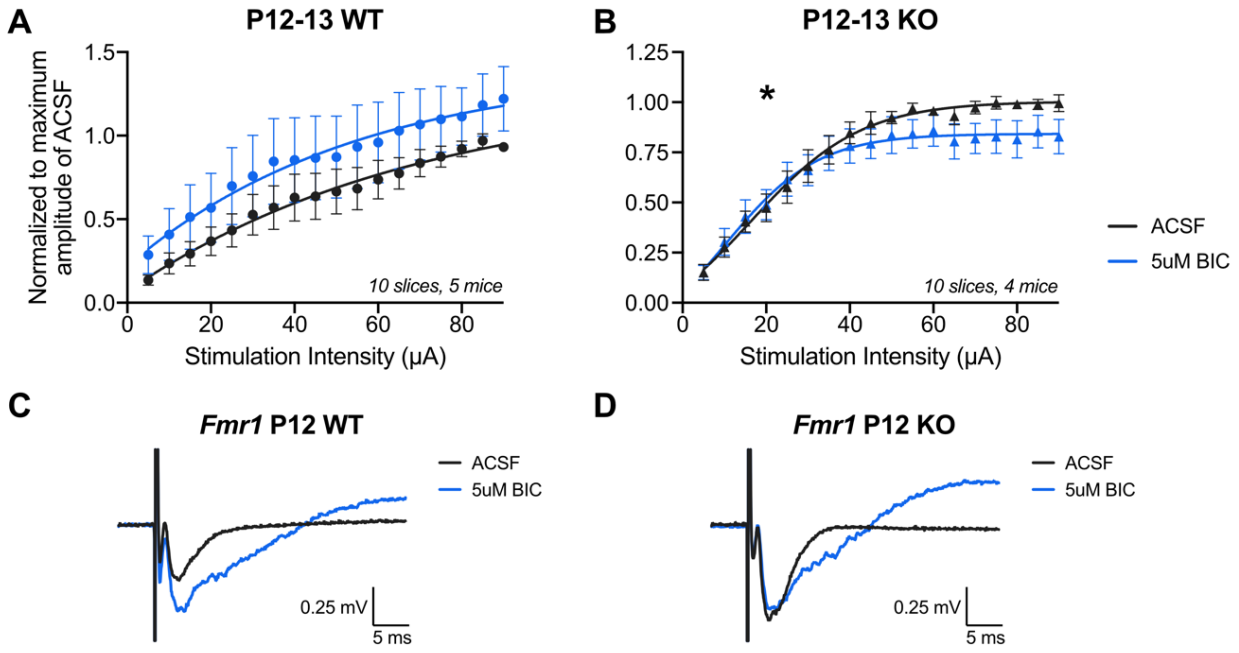

Supplemental Figure 2. The $GABA_AR$ antagonist bicuculline (BIC) also elicits I-O curve responses similar to PTX in P12-13 *Fmr1* KO mice. (A-B) I-O curves from MEA field recordings for P12-13 WT and KO mice were analyzed before and after 5 μM BIC, and normalized to the maximum amplitude in ACSF and fit with sigmoidal curves. (A) WT mice show unaltered differences in I-O curves to BIC (2-way repeated measures ANOVA [mixed-effects model], stimulation intensity × ACSF/BIC, $F_{(19,336)} = 0.1306$, $p > 0.9999$). (B) *Fmr1* KO mice exhibited significantly different I-O curve responses, with decreased fEPSP amplitudes following BIC ($F_{(19,341)} = 1.652$, $p = 0.0429$). (C-D) Representative traces from at 60 μA stimulation. * $p < 0.05$.

	Genotype (n = cells/mice)	Amplitude (pA)	Frequency (Hz)	Weighted Decay τ (ms)
P9-10	WT (22/9)	24.01± 2.18	0.56 ± 0.10	25.42 ± 2.12
	KO (24/7)	23.07 ± 1.46	0.47 ± 0.07	23.19 ± 1.57
		p = 0.7192	*p* = 0.4478	*p* = 0.3976
P12-13	WT (22/9)	20.20 ± 0.98	1.63 ± 0.12	16.86 ± 1.06
	KO (21/8)	20.68 ± 1.52	1.97 ± 0.16	16.75 ± 0.87
		p = 0.7881	***p* = 0.0634**	*p* = 0.9381
P15-16	WT (25/10)	21.36 ± 0.96	4.49 ± 0.32	11.55 ± 0.37
	KO (21/7)	21.16 ± 0.78	4.33 ± 0.28	11.41 ± 0.32
		p = 0.8778	*p* = 0.7214	*p* = 0.7894
P21-25	WT (20/10)	24.70 ± 1.44	6.65 ± 0.34	10.08 ± 0.43
	KO (21/10)	23.33 ± 1.36	7.50 ± 0.39	9.77 ± 0.23
		p = 0.4919	*p* = 0.1086	*p* = 0.5206

Supplemental Table 1. Summary of sIPSC median amplitudes, frequency and weighted decay τ. All values are mean ± SEM. Student's t test or Mann-Whitney was performed for each age, with p values listed.

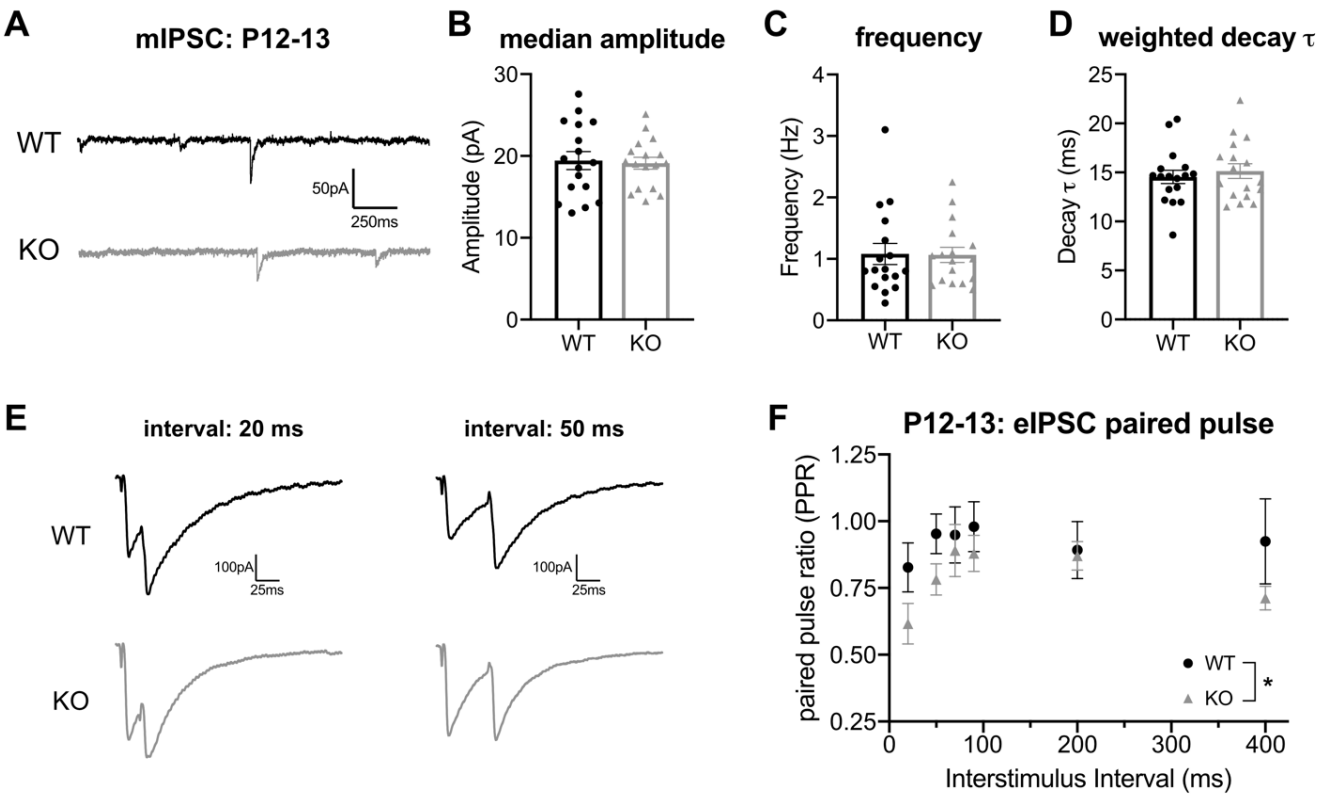

Supplemental Figure 3. Altered presynaptic regulation of inhibitory transmission in L2/3 pyramidal neurons of P12 *Fmr1* KO mice in the auditory cortex. (A-D) mIPSC analysis of L2/3 pyramidal neurons in the auditory cortex. (A) Representative mIPSC traces. (B-D) mIPSC amplitude, frequency (WT: 1.080 ± 0.1712 Hz, KO: 1.065 ± 0.1225 Hz, p = 0.6768), and weighted decay τ are unaltered in P12-13 *Fmr1* KO mice. N = 17 cells/5 WT mice and 17 cells/5 KO mice. (E-F) Paired-pulse ratio analysis of eIPSC at P12-13. (E) Representative traces from interstimulus intervals of 20 and 50 ms. (F) *Fmr1* KO mice have significantly different eIPSC paired-pulse ratios compared to WT mice, with more depressed PPR values (2-way ANOVA, genotype effect, $F_{(1,198)} = 6$, p = 0.012). N = 16 cells/3 WT mice and 19 cells/3 KO mice. * p < 0.05.

		Amplitude (pA)			Weighted decay τ (ms)		
	Geno-type (cells/mice)	ACSF	ZOLP	*p*-value	ACSF	ZOLP	*p*-value
P9-10	WT (12/6)	25.61 ± 3.43	22.87 ± 1.85	0.4866	22.79 ± 2.92	31.6 ± 2.77	0.0041
	KO (14/5)	23.4 ± 2.28	23.85 ± 2.25	0.856	22.12 ± 2.14	31.39 ± 2.43	0.0085
P12-13	WT (9/5)	21.33 ± 1.55	23.08 ± 1.81	0.114	16.54 ± 0.95	22.58 ± 2.16	0.0133
	KO (11/6)	23.18 ± 2.49	28.03 ± 2.38	0.0046	18.47 ± 1.33	22.39 ± 1.63	0.0074
P15-16	WT (10/5)	24.61 ± 1.07	29.96 ± 1.58	0.0018	12.13 ± 0.62	15.5 ± 0.59	< 0.0001
	KO (13/6)	21.88 ± 0.80	25.61 ± 0.83	0.0015	11.42 ± 0.40	15.54 ± 0.37	< 0.0001
P21-25	WT (10/6)	29.11 ± 1.72	31.77 ± 2.14	0.0068	9.47 ± 0.33	12.31 ± 0.42	< 0.0001
	KO (10/6)	25.54 ± 1.67	27.76 ± 1.54	0.1934	9.38 ± 0.25	12.69 ± 0.53	< 0.0001

Supplemental Table 2. Summary of sIPSC pharmacological sensitivity to zolpidem in the auditory cortex. Group mean ± SEM reported for median amplitude and weighted decay τ for ACSF and ZOLP for each age. The *p* values are listed from paired t test or Wilcoxon matched-pairs signed rank.

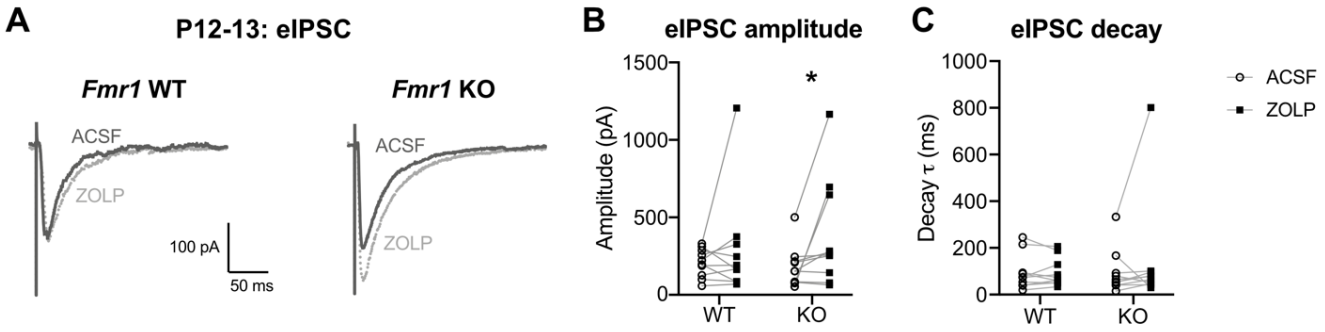

Supplemental Figure 4. *Fmr1* P12 KO mice exhibit enhanced postsynaptic zolpidem (ZOLP) sensitivity. The effect of zolpidem (100 nM) was evaluated on eIPSCs to identify whether the enhanced ZOLP sensitivity measured in sIPSCs was postsynaptically related. (A) Representative eIPSC traces from L2/3 pyramidal neurons following L4 stimulation, before and after zolpidem. (B) *Fmr1* KO mice at P12 had significant increases in eIPSC amplitude following ZOLP (KO-ACSF: 177.24 ± 41.69 pA; KO-ZOLP: 386.37 ± 109.77 pA; $p = 0.0371$) compared to WT mice (WT-ACSF: 207.66 ± 29.06 pA; WT-ZOLP: 291.76 ± 106.60 pA; $p = 0.6250$). (C) No significant changes in weighted decay τ occurred in neither WT nor KO following ZOLP. N = 10 cells/3 WT mice and 10 cells/3 KO mice. Wilcoxon matched-pairs signed rank. * $p < 0.05$.

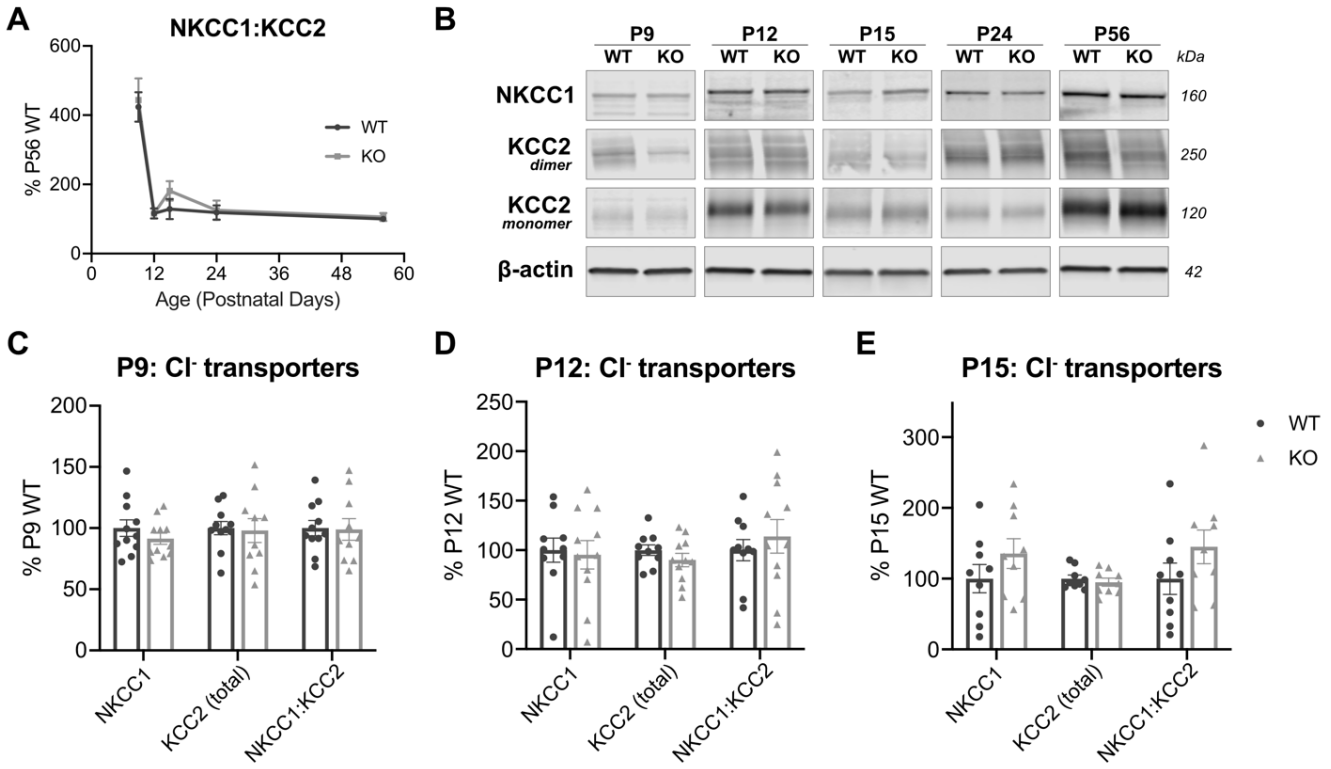

Supplemental Figure 5. *Fmr1* KO and WT mice exhibit similar developmental expressions of chloride transporters in the auditory cortex. (A) The developmental expression of NKCC1:KCC2 plotted with all timepoints normalized to P56 WT to analyze developmental expression, exhibiting a strong age-dependent downregulation of relative NKCC1:KCC2 levels (2-way ANOVA, age, $F_{(4,104)} = 51.04$, $p < 0.0001$). (B) Representative western blots of chloride transporters with β-actin used as loading controls. (C-E) Western blot analysis of membrane-bound NKCC1, total KCC2 (both dimer and monomer levels), and NKCC1:KCC2 in the auditory cortex, normalized relative to age-matched littermates. No differences were observed in the levels of individual transporters or the ratio at (C) P9 (n = 11 WT, 10 KO), (D) P12 (n = 10, 11), or (E) P15 (n = 9, 9). No differences observed at either P24 (n = 11, 10) or P56 (n = 18, 15), data not shown.

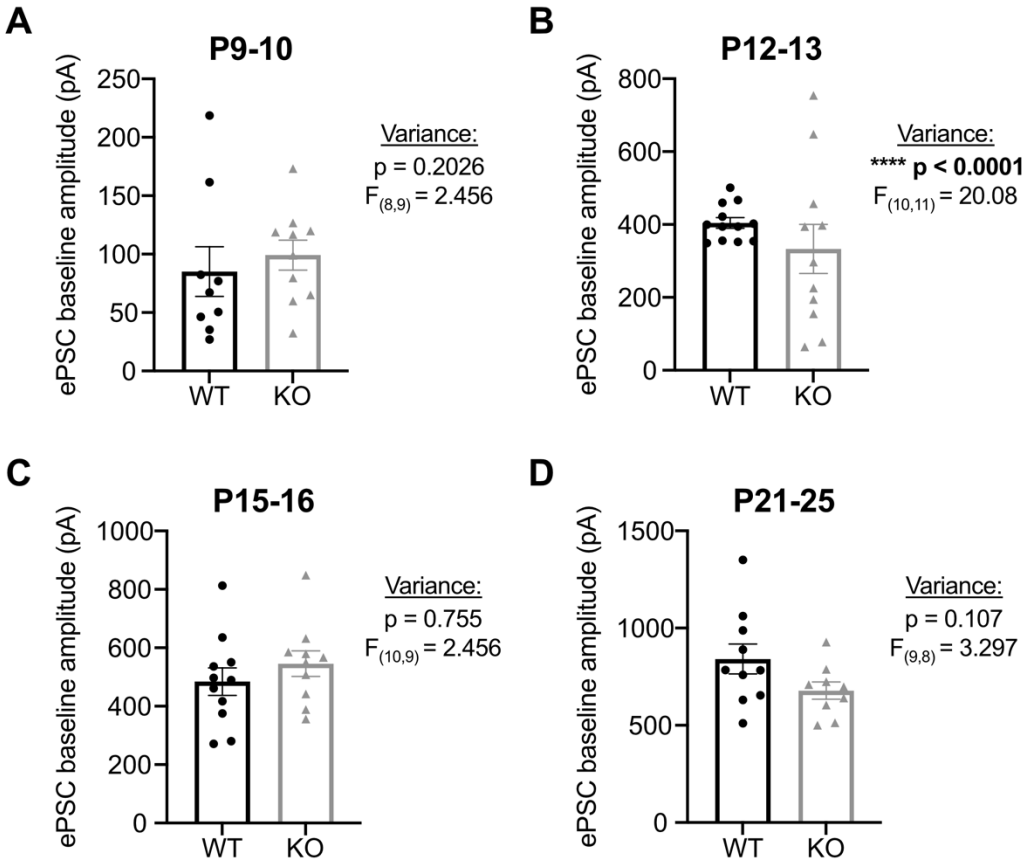

Supplemental Figure 6. *Fmr1* KO mice exhibit significantly greater variability in the average baseline evoked postsynaptic current (ePSC) response at P12. (A-D) The average ePSC amplitude was calculated for each cell from the baseline recordings of ePSC-LTP experiments in Figure 8. While no difference was observed in the average amplitudes of ePSCs in L2/3 pyramidal neurons following L4 stimulation across the developmental ages, (B) P12 KO mice exhibited significantly increased variability in the raw amplitudes of the synaptic responses (WT: 404.3 ± 14.42 pA; KO: 333.1 ± 67.51. The number of cells and mice analyzed for each age and genotype are reported in Figure 8. **** $p < 0.0001$

Supplemental Figure 7. Sample of full scan western blots for each of the developmental ages. Each blot was loaded with alternating lanes of WT and *Fmr1* KO mice auditory cortex lysates. For direct within-age evaluations (Fig. 3D-G; Supplemental Fig. 5C-E), target proteins were normalized to their respective β-actin and expressed as a percentage of mean age-matched WT samples for each western blot membrane. For developmental expression profiles (Fig. 3A-C; Supplemental Fig. 5A), each sample was expressed as a percentage of the mean P56 WT samples run on the sample membrane. The P56 WT samples used in P9, P12, and P15 membranes (A-C) were originally ran and analyzed run on the P56 only blot (E). Bio-Rad Precision Plus Protein Kaleidoscope and Invitrogen MagicMark were used as ladders for detection within the 20-250 kD and 20-220 kD range, respectively. Membranes were cut (dotted white lines indicate the location of the cut) and probed with multiple antibodies as indicated (NMDA receptor subunit, GluN1, was probed but not analyzed and included for this article). Grayscale images show the bands from the individual channels. Orange and purple boxes show the cropped regions used for representative bands in the main article figures.

See following pages for Supplemental Fig. 7A-E

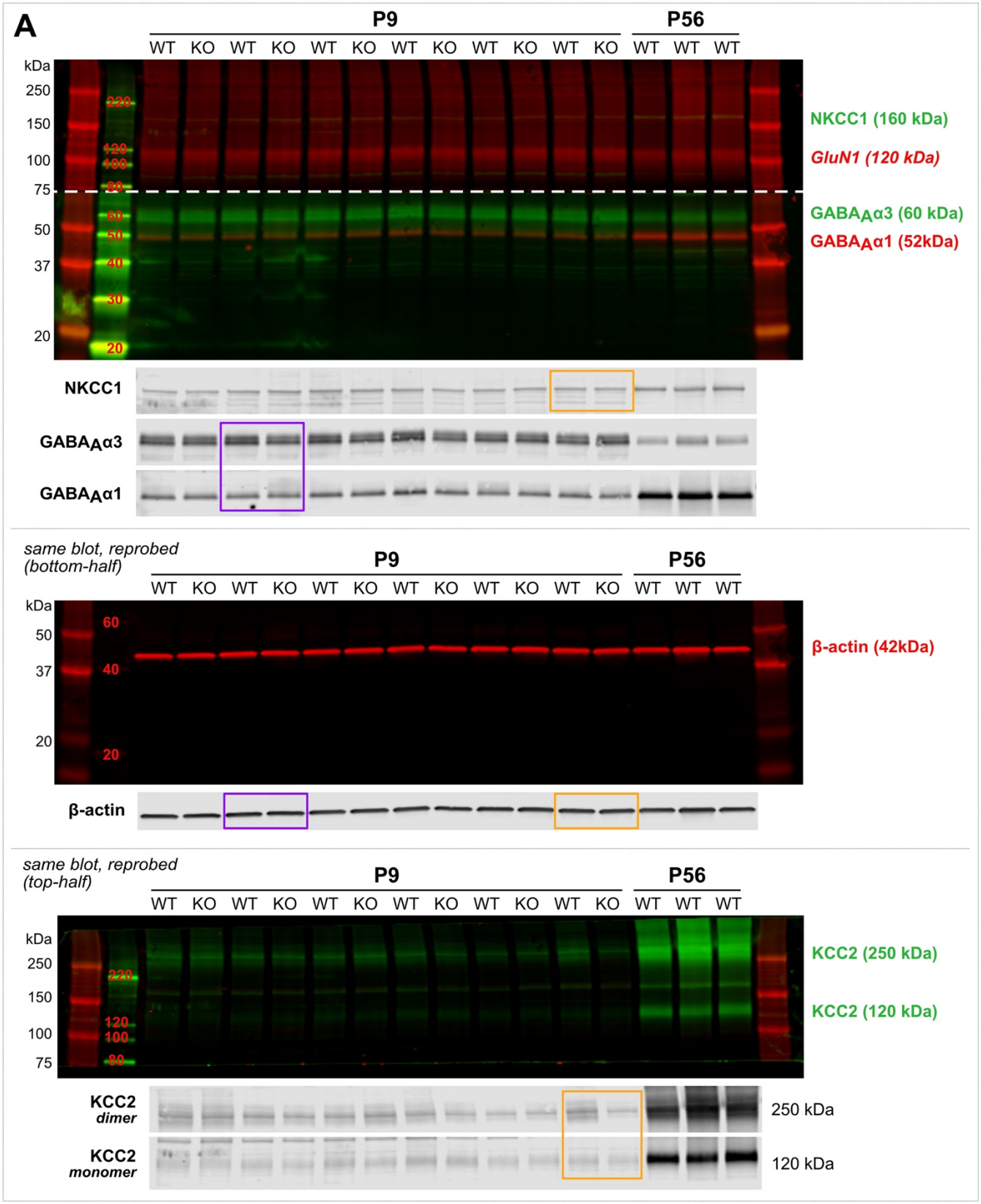
A
P9
P56
WT KO WT KO WT KO WT KO WT KO WT KO WT WT WT
kDa
250
150
100
75
50
37
20
220
120
100
80
60
50
40
30
20
NKCC1 (160 kDa)
GluN1 (120 kDa)
GABAAα3 (60 kDa)
GABAAα1 (52kDa)
NKCC1
GABAAα3
GABAAα1
same blot, reprobed (bottom-half)
β-actin (42kDa)
β-actin
same blot, reprobed (top-half)
KCC2 (250 kDa)
KCC2 (120 kDa)
KCC2 dimer
KCC2 monomer
250 kDa
120 kDa

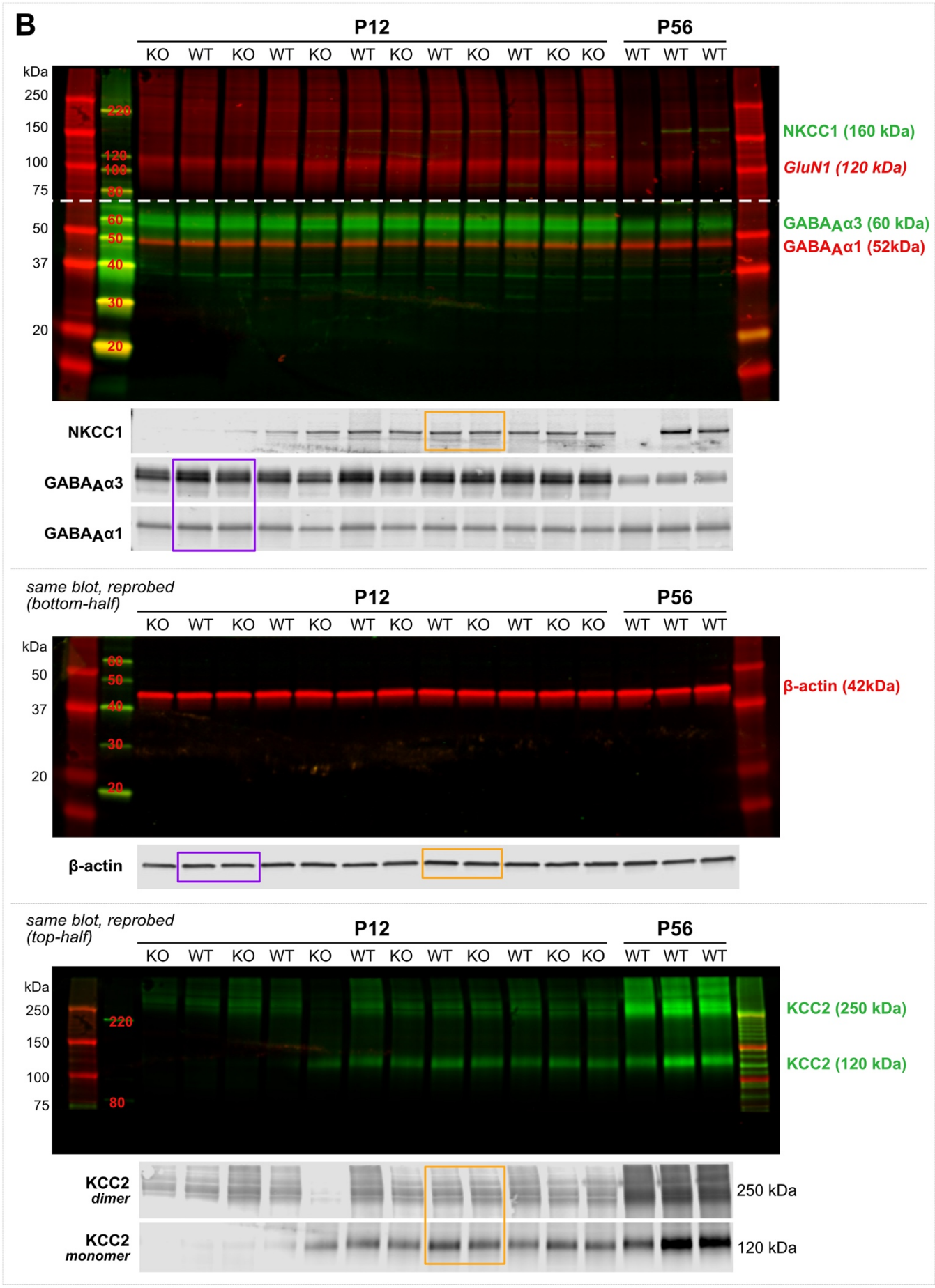
B
P12
P56
KO WT KO WT KO WT KO WT KO WT KO KO WT WT WT
kDa
250
150
100
75
50
37
20
220
120
100
80
60
50
40
30
20
NKCC1 (160 kDa)
GluN1 (120 kDa)
GABAAα3 (60 kDa)
GABAAα1 (52kDa)
NKCC1
GABAAα3
GABAAα1
same blot, reprobed (bottom-half)
P12
P56
KO WT KO WT KO WT KO WT KO WT KO KO WT WT WT
kDa
50
37
20
60
50
40
30
20
β-actin (42kDa)
β-actin
same blot, reprobed (top-half)
P12
P56
KO WT KO WT KO WT KO WT KO WT KO KO WT WT WT
kDa
250
150
100
75
220
80
KCC2 (250 kDa)
KCC2 (120 kDa)
KCC2 dimer
KCC2 monomer
250 kDa
120 kDa

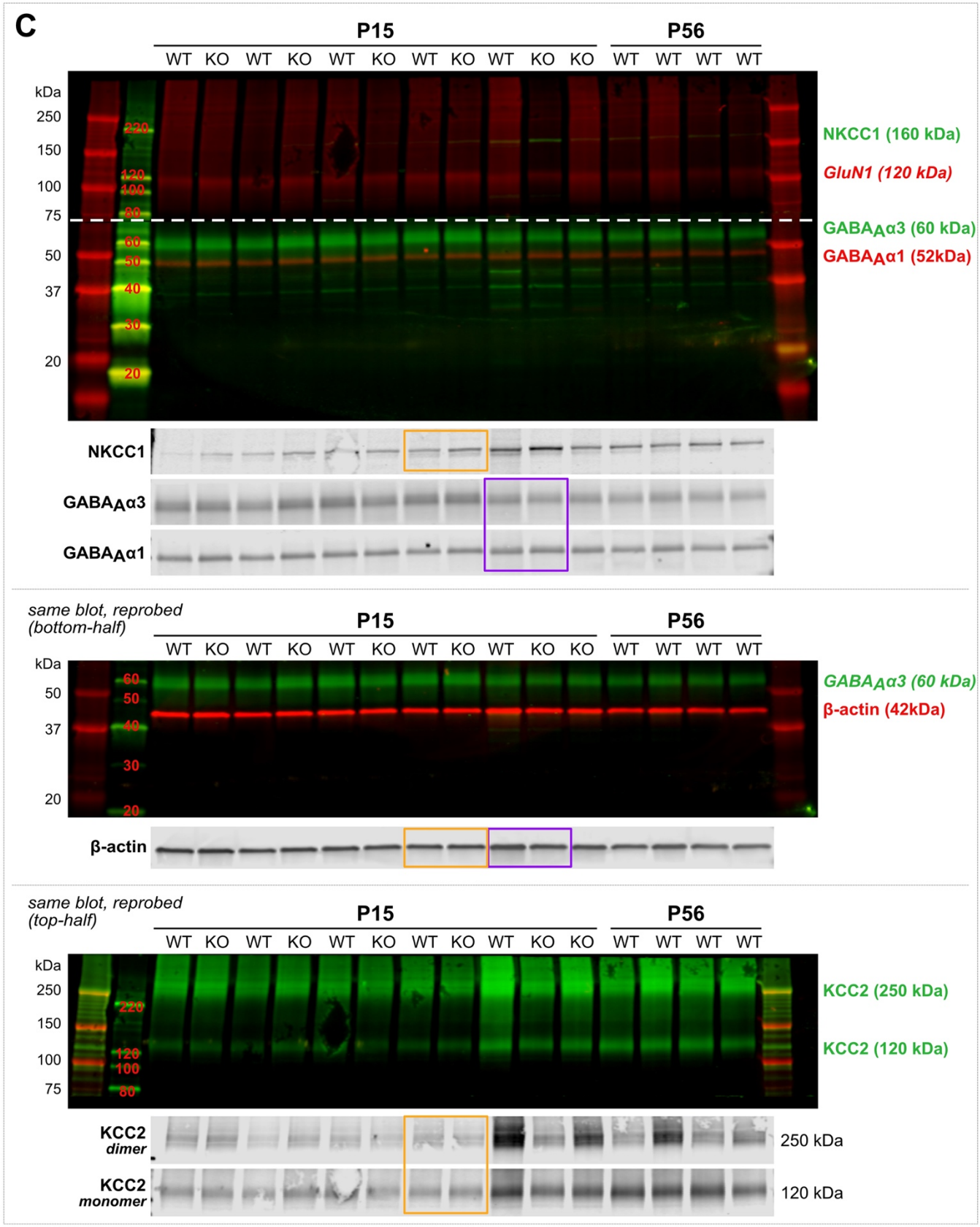
C
P15
P56
WT KO WT KO WT KO WT KO WT KO KO WT WT WT WT
kDa
250
150
100
75
50
37
20
220
120
100
80
60
50
40
30
20
NKCC1 (160 kDa)
GluN1 (120 kDa)
GABAAα3 (60 kDa)
GABAAα1 (52kDa)
NKCC1
GABAAα3
GABAAα1
same blot, reprobed (bottom-half)
P15
P56
WT KO WT KO WT KO WT KO WT KO KO WT WT WT WT
kDa
50
37
20
60
50
40
30
20
GABAAα3 (60 kDa)
β-actin (42kDa)
β-actin
same blot, reprobed (top-half)
P15
P56
WT KO WT KO WT KO WT KO WT KO KO WT WT WT WT
kDa
250
150
100
75
220
120
100
80
KCC2 (250 kDa)
KCC2 (120 kDa)
KCC2 dimer
KCC2 monomer
250 kDa
120 kDa

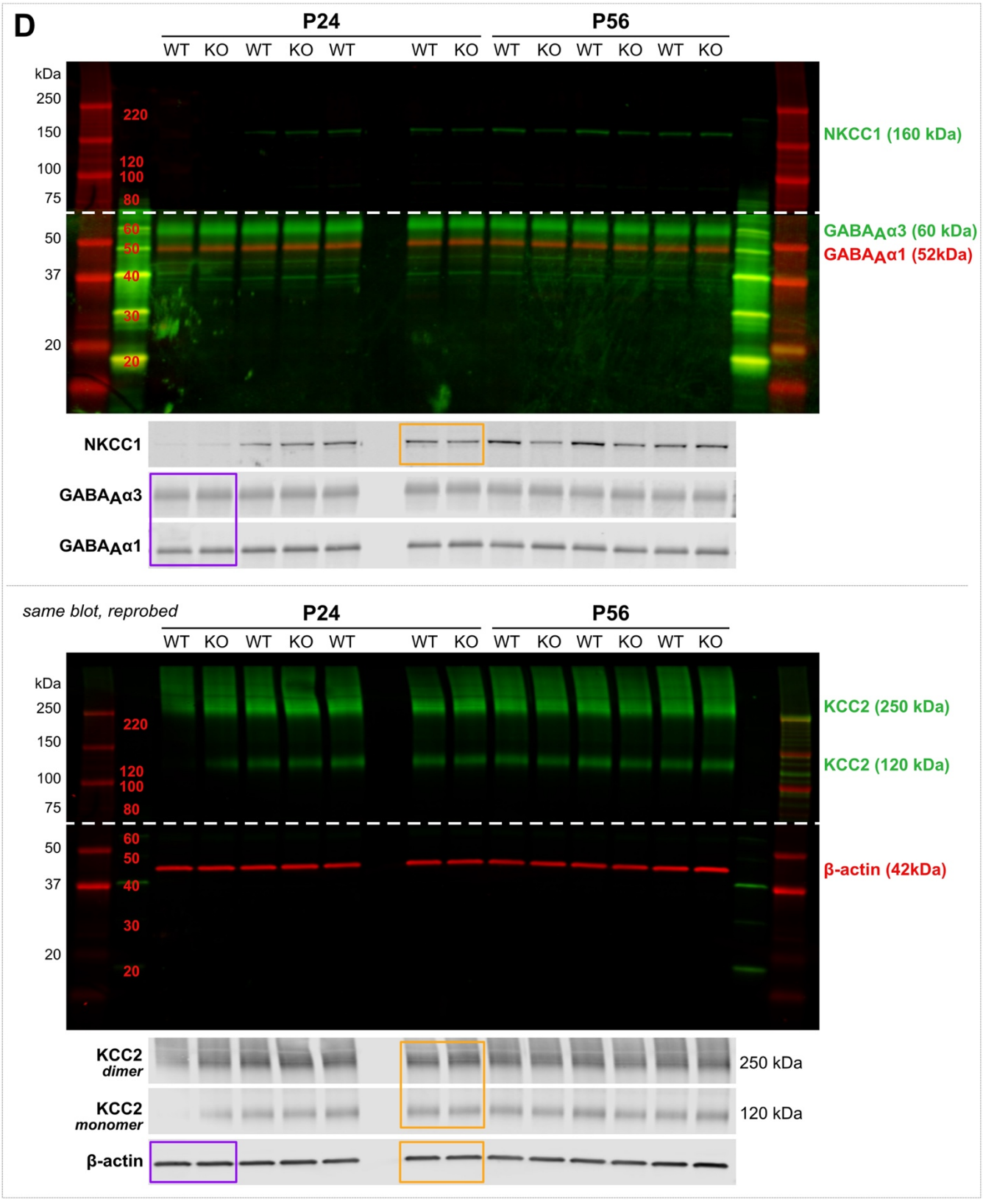
D
P24
P56
WT KO WT KO WT WT KO WT KO WT KO WT KO
kDa
250
150
100
75
50
37
20
220
120
100
80
60
50
40
30
20
NKCC1 (160 kDa)
GABAAα3 (60 kDa)
GABAAα1 (52kDa)
NKCC1
GABAAα3
GABAAα1
same blot, reprobed
P24
P56
WT KO WT KO WT WT KO WT KO WT KO WT KO
kDa
250
150
100
75
50
37
20
220
120
100
80
60
50
40
30
20
KCC2 (250 kDa)
KCC2 (120 kDa)
β-actin (42kDa)
KCC2 dimer
KCC2 monomer
β-actin
250 kDa
120 kDa

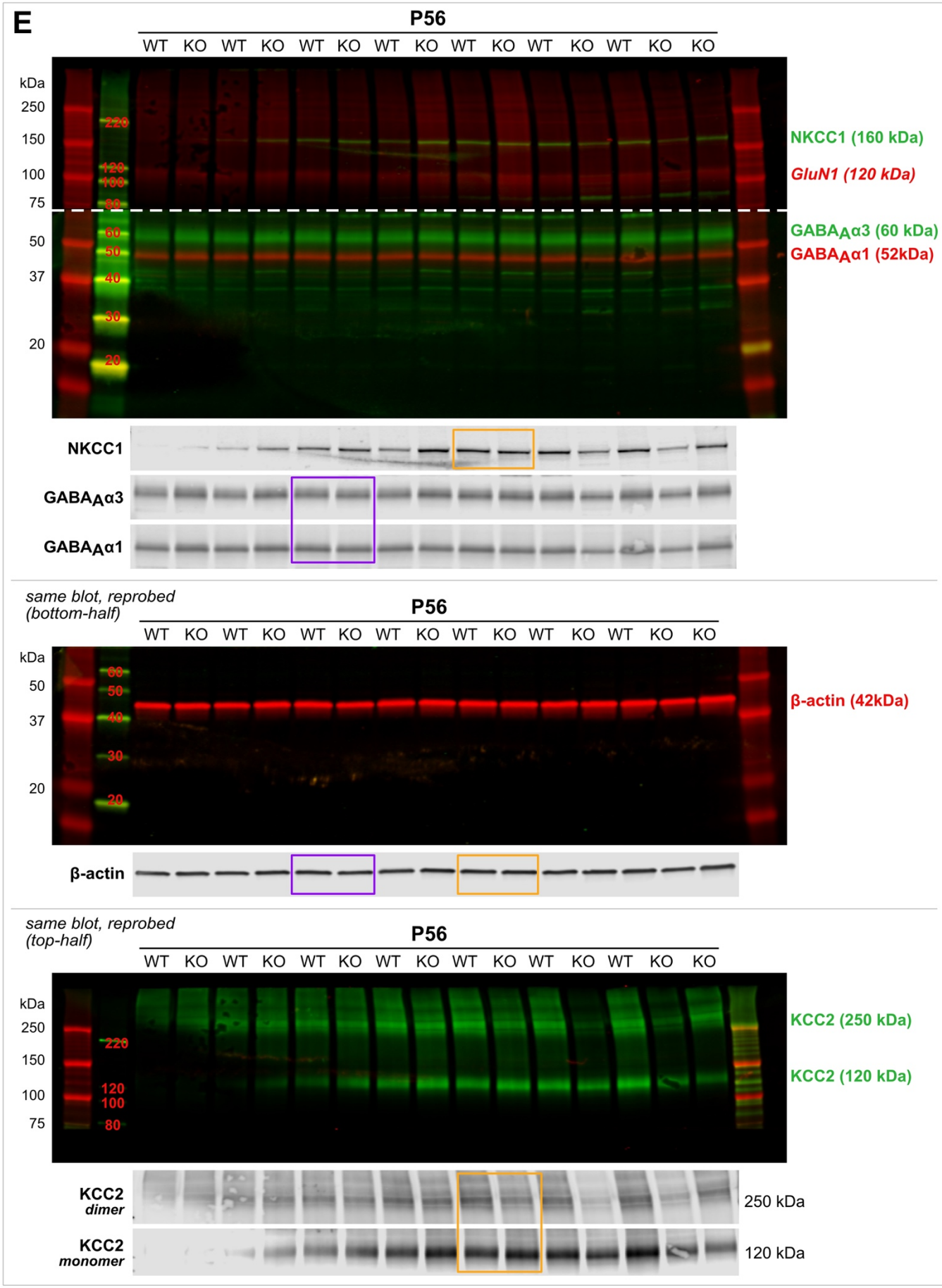
E
P56
WT KO WT KO WT KO WT KO WT KO WT KO WT KO KO
kDa
250
150
100
75
50
37
20
220
120
100
80
60
50
40
30
20
NKCC1 (160 kDa)
GluN1 (120 kDa)
GABAAα3 (60 kDa)
GABAAα1 (52kDa)
NKCC1
GABAAα3
GABAAα1
same blot, reprobed (bottom-half)
P56
WT KO WT KO WT KO WT KO WT KO WT KO WT KO KO
kDa
50
37
20
60
50
40
30
20
β-actin (42kDa)
β-actin
same blot, reprobed (top-half)
P56
WT KO WT KO WT KO WT KO WT KO WT KO WT KO KO
kDa
250
150
100
75
220
120
100
80
KCC2 (250 kDa)
KCC2 (120 kDa)
KCC2 dimer
KCC2 monomer
250 kDa
120 kDa